Renormalization-group results for lattice surface models

1995 J. Phys. A: Math. Gen. 28 867

(http://iopscience.iop.org/0305-4470/28/4/013)

J. Phys. A: Math. Gen. 28 (1995) 867–877. Printed in the UK

Renormalization-group results for lattice surface models

Emilio N M Cirillo and Giuseppe Gonnella

Dipartimento di Fisica dell'Università di Bari and Istituto Nazionale di Fisica Nucleare, Sezione di Bari, via Amendola 173, I-70126 Bari, Italy

Received 10 November 1994

Abstract. We study the phase diagram of statistical systems of closed and open interfaces built on a cubic lattice. Interacting closed interfaces can be written as Ising models, while open surfaces can be written as $Z(2)$ gauge systems. When the open surfaces reduce to closed interfaces with few defects, the gauge model can be also written as an Ising spin model. We apply the lower bound renormalization group (LBRG) transformation introduced by Kadanoff (*1975 Phys. Rev. Lett. 34 1005*) to study the Ising models describing closed and open surfaces with few defects. In particular, we have studied the Ising-like transition of self-avoiding surfaces between the random isotropic phase and the phase with broken global symmetry at varying values of the mean curvature. Our results are compared with previous numerical work. The limits of the LBRG transformation in describing regions of the phase diagram where non-ferromagnetic ground states are relevant are also discussed.

1. Introduction

In this paper we will apply a renormalization-group transformation to study the phase diagram of interface models built on a cubic lattice. Fluid interfaces in 3D statistical systems are the subject of much current research [1]. They provide useful descriptions of experimental systems such as mixtures of oil, water and surfactant, or aqueous solutions of surfactant [2]. In ternary mixtures the surfactant forms monolayered interfaces between oil and water; in aqueous solutions bilayered membranes are typical constituents of biological cells. The properties of these systems at low surfactant concentrations are relevant for both practical and theoretical reasons. For example, in ternary mixtures, a middle phase [3] coexisting with oil-rich and water-rich phases is considered very appealing for applications [4], due to the very low surface tension values between the coexisting phases. From a theoretical point of view, dilute interfaces can be seen as experimental realizations of random surface models where self-avoidness is the only relevant interaction [5].

The typical lack of topological constraints on the physical configurations suggests the use of lattice models to describe ensembles of fluid surfaces. First consider the case of closed interfaces without defects such as holes or seams. Closed interfaces can be described in Ising models as the boundaries separating domains of opposite spins, which, in the identification with ternary mixtures, can represent oil and water. The interfaces are built on the dual lattice, and, for a given spin configuration $\{\sigma_i\}$, have a total area $\mathcal{S} = \sum_{\langle ij \rangle}(1 - \sigma_i\sigma_j)/2$, where the sum is over all nearest-neighbour pairs in the original lattice. Other surface energies can be considered by introducing further spin interactions. Surfaces where curvature and intersections [6] are also weighted can be represented by a generalization of the Ising model

0305-4470/95/040867+11$19.50

defined by the Hamiltonian [7–9]

$$H = \mathcal{J}_1 \sum_{\langle ij \rangle} \sigma_i \sigma_j + \mathcal{J}_2 \sum_{\langle\langle ij \rangle\rangle} \sigma_i \sigma_j + \mathcal{J}_4 \sum_{i \square_k^j} \sigma_i \sigma_j \sigma_k \sigma_l \tag{1}$$

where the three sums are over the nearest, next-to-the-nearest neighbours and plaquettes of a cubic lattice, respectively. Here and in the following, our definitions of the Hamiltonian will always include the factor $-\beta$. The parameters $\mathcal{J}_1, \mathcal{J}_2$ and $\mathcal{J}_4$ can be expressed in terms of the surface parameters β_S, β_C and β_L [9] representing, respectively, the energy cost for an elementary area (one plaquette on the dual lattice), for two plaquettes at right angles, and for four plaquettes with a common bond [10]. A positive β_C favours flat configurations; it corresponds to a mean curvature energy, which has been proved to be an useful phenomenological parameter for describing fluid interfaces [11]. The term proportional to β_L can mimic the self-avoidness interaction in the limit $\beta_L \to \infty$, when surfaces touching each other along some contour are forbidden. The relations between spin and surface parameters are

$$\mathcal{J}_1 = \tfrac{1}{2}(\beta_S + \beta_L) + \beta_C \qquad \mathcal{J}_2 = -\tfrac{1}{8}\beta_L - \tfrac{1}{4}\beta_C \qquad \mathcal{J}_4 = -\tfrac{1}{8}\beta_L + \tfrac{1}{4}\beta_C \,. \tag{2}$$

The phase diagram of the model (1) was studied by mean-field and numerical simulations in [8, 9]. It exhibits many properties relevant for real systems, as also discussed in [12].

If one wishes to consider the effects of defects in fluid interfaces, ensembles of open surfaces have to be introduced. A simple lattice realization of open surfaces [13] is given by the self-dual $Z(2)$ gauge model [14]. Here two-value variables $\{U_{ij}\}$ are defined on the bonds of a cubic lattice. One says that the plaquette dual to the bond (ij) is occupied by some surface if $U_{ij} = -1$; it is not occupied if $U_{ij} = 1$. Therefore a given $\{U_{ij}\}$ configuration corresponds on the dual lattice to a surface configuration with area $\mathcal{S} = \sum_{\langle ij \rangle}(1 - U_{ij})/2$. A bond on the dual lattice can be said to belong to some defect if an odd number of the dual plaquettes sharing that bond is occupied by some surface. Defects defined in this way can be counted by considering the product of U_{ij} over the bonds of each plaquette in the original lattice. It is easy to recognize that the total length of defects will correspond to the quantity $\mathcal{D} = \sum_{i \square_k^j}(1 - U_{ij}U_{jk}U_{kl}U_{li})/2$ [13]. Therefore the self-dual $Z(2)$ gauge model with Hamiltonian given by

$$H = \beta_M \sum_{\langle ij \rangle} U_{ij} + \beta_G \sum_{i \square_k^j} U_{ij}U_{jk}U_{kl}U_{li} \tag{3}$$

describes open surfaces where area and defects are both weighted. Self-duality here [14] means that the model is symmetric with respect to the transformations

$$\beta_M \to \tilde{\beta}_G = -\tfrac{1}{2} \ln \tanh \beta_M \qquad \beta_G \to \tilde{\beta}_M = -\tfrac{1}{2} \ln \tanh \beta_G \,. \tag{4}$$

In the parametrization (3) a large value of β_M favours configurations with small area, while a large value of β_G inhibits defects.

The phase diagram of the self-dual $Z(2)$ gauge model was first analysed in [14, 15]; it has been studied by Monte Carlo simulations in [16]. At small values of β_M—and analogously, by self-duality, at large values of β_G—it can be shown [15, 17] that the model (3) can be expanded as an Ising spin model with an increasing number of interactions. For example, at the second order of the expansion at small β_M the model (3) can be written as

$$H = \mathcal{J}_1 \sum_{\langle ij \rangle} \sigma_i \sigma_j + \mathcal{J}_2 \sum_{\langle\langle ij \rangle\rangle} \sigma_i \sigma_j + \mathcal{J}_4 \sum_{i \square_k^j} \sigma_i \sigma_j \sigma_k \sigma_l + \mathcal{J}_6 \sum_{\text{cor}} \sigma_i \sigma_j \sigma_k \sigma_l \tag{5}$$

Table 1. The coordinates of the fixed point related to the F-AF-P transitions are reported for the value $p = p_c^*$ which maximizes the free energy of the critical F-P fixed point (C). The other symbols (F), (AF), (P), (AC), (D) and (L) denote, respectively, the low-temperature ferromagnetic and antiferromagnetic fixed points, the high-temperature, the critical AF-P, the discontinuity fixed point between the AF and F phases, and the fixed point on the manifold separating the domains of attraction of the fixed points (C) and (D) (on the hypersurface limiting the F phase). The two squares on the left represent two parallel faces of an elementary cube of the lattice. The dots represent the spins taking part in a given interaction. In [19] the value of p maximizing the critical F-P fixed-point free energy has been found to be $p = 0.403\,43$. This fixed point is symmetric (in the sense explained in the main text) and the two-spin, four-spin, six-spin and eight-spin coordinates are 0.020 97, 1.96×10^{-4}, -7.69×10^{-5} and 2.15×10^{-5}, respectively.

K_2^*	−0.093 71	−0.094 47	−0.042 31	−0.020 96	−0.115 50	-1.19×10^{-3}	−0.022 93
K_3^*	−0.093 71	−0.094 47	−0.129 74	−0.020 96	−0.017 20	−0.113 42	−0.017 91
K_4^*	-9.99×10^{-3}	−0.010 18	-6.54×10^{-3}	-1.97×10^{-4}	-2.65×10^{-4}	-6.94×10^{-7}	-1.96×10^{-4}
K_5^*	-9.99×10^{-3}	−0.010 18	-2.73×10^{-3}	-1.97×10^{-4}	-2.65×10^{-4}	-1.23×10^{-5}	-2.31×10^{-4}
K_6^*	-9.99×10^{-3}	−0.010 18	-6.55×10^{-3}	-1.97×10^{-4}	-3.07×10^{-3}	-6.95×10^{-7}	-1.48×10^{-4}
K_7^*	-9.99×10^{-3}	−0.010 18	-2.72×10^{-3}	-1.97×10^{-4}	-3.07×10^{-3}	-1.23×10^{-5}	-1.82×10^{-4}
K_8^*	-9.99×10^{-3}	−0.010 18	-4.63×10^{-3}	-1.97×10^{-4}	-2.65×10^{-4}	-1.65×10^{-4}	-2.67×10^{-4}
K_9^*	-9.99×10^{-3}	−0.010 18	-6.59×10^{-3}	-1.97×10^{-4}	-2.51×10^{-2}	-6.94×10^{-7}	-1.73×10^{-5}
K_{10}^*	-4.68×10^{-3}	-4.76×10^{-3}	-8.98×10^{-4}	-7.72×10^{-5}	-5.59×10^{-4}	-2.37×10^{-7}	-7.84×10^{-5}
K_{11}^*	-4.68×10^{-3}	-4.76×10^{-3}	-9.00×10^{-4}	-7.72×10^{-5}	-2.82×10^{-4}	-2.37×10^{-7}	-7.56×10^{-5}
K_{12}^*	-4.68×10^{-3}	-4.76×10^{-3}	-1.08×10^{-3}	-7.72×10^{-5}	-5.59×10^{-4}	-6.47×10^{-6}	-8.06×10^{-5}
K_{13}^*	-7.69×10^{-3}	-7.88×10^{-3}	-5.96×10^{-7}	-2.15×10^{-5}	-3.04×10^{-4}	-3.42×10^{-7}	-2.15×10^{-5}

where the interactions are between nearest neighbours, next-to-the-nearest neighbours, the four spins of a plaquette and the four spins of a corner (see table 1). The coupling constants $\mathcal{J}_1$, $\mathcal{J}_2$, $\mathcal{J}_4$ and $\mathcal{J}_6$ can be expressed in terms of the constants β_G and β_M as follows:

$$\begin{aligned}
\mathcal{J}_1 &= \tilde{\beta} - 4(\tanh\beta_M)^6[3\cosh 2\tilde{\beta}\sinh 2\tilde{\beta} + (\cosh 2\tilde{\beta})^2\sinh 2\tilde{\beta}] \\
\mathcal{J}_2 &= 2(\tanh\beta_M)^6[(\sinh 2\tilde{\beta})^2 + \cosh 2\tilde{\beta}(\sinh 2\tilde{\beta})^2] \\
\mathcal{J}_4 &= 2(\tanh\beta_M)^6(\sinh 2\tilde{\beta})^2 \\
\mathcal{J}_6 &= -\tfrac{1}{2}(\tanh\beta_M)^6(\sinh 2\tilde{\beta})^3
\end{aligned} \tag{6}$$

where

$$\tilde{\beta} = -\tfrac{1}{2}\ln\tanh\left[\beta_G + (\tanh\beta_M)^4\right]. \tag{7}$$

The spin representation has the advantage that it can be more easily studied [18].

In this paper we will apply the so-called lower-bound renormalization group (LBRG) transformation first proposed by Kadanoff [19] to study the phase diagram of the models (1) and (3) as given in the approximation (5). The LBRG transformation can be conveniently applied to cases where all the interaction is in an elementary cell of the lattice, as it is in the models (1) and (5). The convenience is appreciable especially in $D = 3$ where other RG transformations would be much more difficult from a computational point of view.

The LBRG transformation produces a lower bound to the free energy which can be maximized by conveniently fixing a variational parameter. Its application to various models generally gives very accurate estimates of critical exponents [20]. For example, in the 2D Ising model it predicts the inverse critical temperature $\beta_{crit} = 0.458$ ($\beta_{crit}^{Onsager} = 0.4407$), and the exponent $\nu = 0.999$ ($\nu^{Onsager} = 1$) [21]. The drawback of the LBRG transformation

is that it preserves the nature of the ground states only in the ferromagnetic region, so that it can be reliably applied in a limited region of the phase diagram.

We will describe the LBRG transformation in section 2. In section 3 we will show the results obtained by applying the LBRG transformation to the models (1) and (3), (5). In particular, in model (1), the self-avoidness limit is examined for different values of the curvature β_C. A discussion of our results will follow in section 4.

2. The LBRG transformation

$$e^{H'(\sigma',\mathcal{J}')} = \sum_{\sigma} \mathcal{P}(\sigma',\sigma)\, e^{H(\sigma,\mathcal{J})} \tag{8}$$

Here $\mathcal{J}$ denotes a set of coupling constants, $\sigma = \{\sigma_1, \ldots \sigma_N\}$ a spin configuration and $H(\sigma, \mathcal{J})$ is the Hamiltonian to be studied; the weight function $\mathcal{P}(\sigma';\sigma)$ defines the renormalized Hamiltonian $H'(\sigma', \mathcal{J}')$ with new spin variables $\sigma'_1, \ldots, \sigma'_{N'}$ $(N' < N)$ and coupling constants $\mathcal{J}'$. The relation $\sum_{\sigma'} \mathcal{P}(\sigma';\sigma) = 1$ ensures that the total free energy is unchanged. In the LBRG transformation [19] the spin σ'_i are defined on cells like those marked by a cross in figure 1; $\mathcal{P}(\sigma',\sigma)$ is chosen as the product over the marked cells of the functions

$$\hat{\mathcal{P}}(\sigma'_i;\sigma_{i,1},\ldots,\sigma_{i,8}) = \frac{\exp[p\sigma'_i(\sigma_{i,1}+\cdots+\sigma_{i,8})]}{2\cosh[p(\sigma_{i,1}+\cdots+\sigma_{i,8})]} \qquad \forall i = 1 \ldots N' \tag{9}$$

with p a real parameter and $\sigma_{i,1}, \ldots \sigma_{i,8}$ the original spins at the vertices of the cube i.

If the original Hamiltonian can be written as $H(\sigma, \mathcal{J}) = \sum \hat{H}(\sigma, \mathcal{K})$, where the sum is over the elementary cubes of the lattice and $\mathcal{K}$ is the set of couplings normalized to a single cell [22], a convenient *moving* of interactions and factors of (9) will give a new Hamiltonian with all the interaction still in a single cell. The renormalized cell Hamiltonian $\hat{H}'(\sigma', \mathcal{K}')$ is given by

$$\exp[\hat{H}'(\sigma'_1,\ldots,\sigma'_8;\mathcal{K}')] = \sum_{\sigma_1,\ldots,\sigma_8} \frac{\exp[p(\sigma'_1\sigma_1+\cdots+\sigma'_8\sigma_8)+8\hat{H}(\sigma_1,\ldots,\sigma_8;\mathcal{K})]}{2\cosh[p(\sigma_1+\cdots+\sigma_8)]}. \tag{10}$$

Since we are interested in studying the phase diagrams of the Ising models (1) and (5) where only even interactions appear, it will be sufficient to consider the transformation of

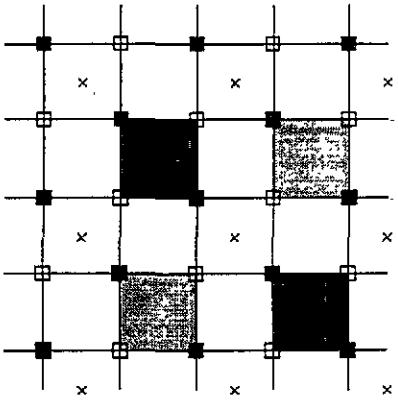

Figure 1. A 2D representation of the LBRG transformation. The crosses indicate the spins σ'; the squares are the original spins σ. The σ-dependent terms in the Hamiltonian and in the weight function are moved into the grey squares. Full and empty squares represent spins of the two original sublattices. In the variant of the LBRG transformation described in section 4 the σ-dependent terms are moved into the dark grey cells of the lattice.

the 14 even couplings (see table 1) which can be defined on a cell of a 3D cubic lattice. One of these couplings is a pure constant, we denote it by $\mathcal{K}_0$; the others are denoted by $\mathcal{K}_i$, $i = 1, \ldots, 13$.

After some algebra one gets from (10) the recursion laws

$$\begin{aligned} \mathcal{K}_0' &= 8\mathcal{K}_0 + \Phi_0(p; \mathcal{K}_1, \ldots, \mathcal{K}_{13}) \\ \mathcal{K}_i' &= \Phi_i(p; \mathcal{K}_1, \ldots \mathcal{K}_{13}) \qquad \forall i = 1, \ldots, 13 \end{aligned} \tag{11}$$

where $\Phi_0, \ldots, \Phi_{13}$ are analytic functions. The critical properties of the system can be then related to the behaviour of the recursion laws close to their fixed points.

The variational nature of the interaction-moving operation was first observed by Kadanoff [23]. A lower bound $f^*(p)$ to the free-energy per site can be calculated by

$$f^*(p) = -\lim_{n\to\infty} \frac{\mathcal{K}_0^{(n)}}{8^n} \tag{12}$$

where $\mathcal{K}_0^{(n)}$ is the value of $\mathcal{K}_0$ after n applications of the LBRG transformation [19]. Following the prescription of [19], the parameter p will be fixed by maximizing the function $f^*(p)$ starting the iterations from the fixed point Hamiltonian with $\mathcal{K}_0 = 0$.

3. Results

Closed interfaces—model (1)

Here the LBRG transformation is applied to calculate the ferromagnetic–paramagnetic (F–P) transition surface in the space $\mathcal{J}_1, \mathcal{J}_2$ and $\mathcal{J}_4$. For completeness, results concerning other transitions, not related to ferromagnetic ordering, will be also given. These results have to be considered with caution since the LBRG transformation, as defined in section 2, does not correctly take in account the structure of not ferromagnetic ground states.

The value of p maximizing the critical fixed-point free energy on the F–P surface is $p_c^* = 0.403\,54$. In table 1 fixed points related to the F, P and AF (antiferromagnetic) phases are reported for the value $p = p_c^*$.

The fixed points (F), (P) and (C) are, respectively, the low-temperature ferromagnetic, the high-temperature and the F–P critical fixed points. The LBRG transformation has already been applied for calculating the exponents of the 3D Ising model in [19], where the optimal value found for p^* is $p = 0.403\,43$. We do not understand the reasons for the discrepancy with our result. The critical fixed point at $p = 0.403\,43$ is reported in the caption of table 1. At $p = p_c^*$ the values of the inverse Ising critical temperature and of the exponent ν are, respectively, $\beta_{crit}^I = 0.239\,25$ and $\nu = 0.6288$. The corresponding values at $p = 0.403\,43$ are $\beta_{crit}^I = 0.239\,23$ and $\nu = 0.6290$; the best estimates [24] are $\beta_{crit}^I = 0.221\,65$ and $\nu = 0.6289 \pm 0.0008$. The fixed point (C) is symmetric in the sense that all the two-spin, the four-spin, etc interactions are equal. This symmetry was assumed in [19], while here we consider recursions in the whole space of couplings. This situation can be compared with the results obtained by applying the LBRG transformation to the 2D Ising model [21]. In $D = 2$ the symmetric fixed point has two relevant eigenvalues with an eigenvector pointing outside the symmetric subspace on the critical surface. Therefore in $D = 2$, differently from the 3D case, the symmetric critical fixed point, which is found to maximize the free energy, cannot be reached starting from non symmetric interactions [21].

The fixed points (AF) and (AC) are the antiferromagnetic counterparts of the fixed points (F) and (C). The fixed point (AC) is on the transition surface between the AF and the P phases; its exponent is $\nu = 0.6349$. This surface intersects the surface $\mathcal{F}$ limiting the

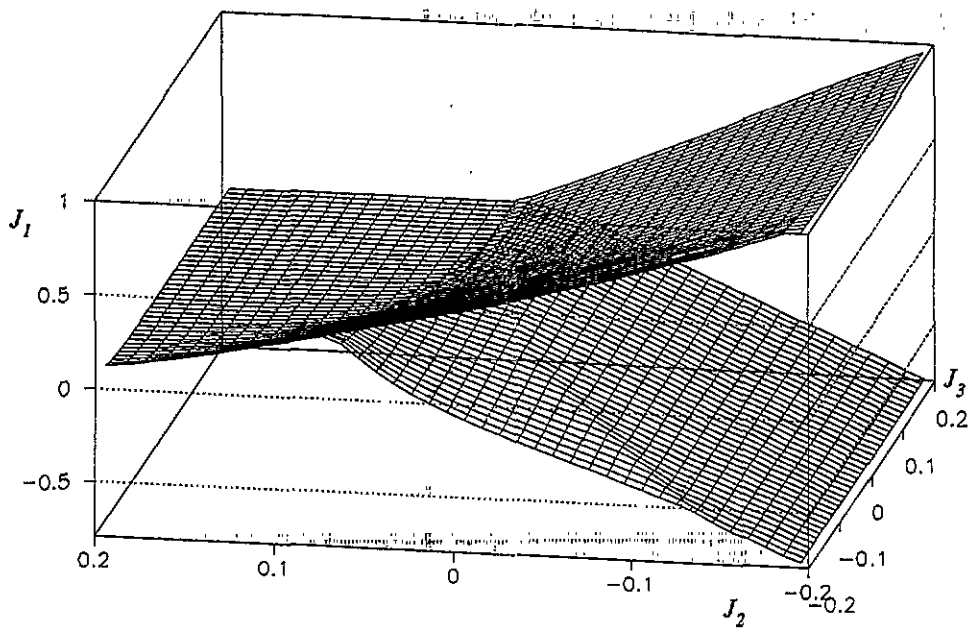

Figure 2. The phase diagram obtained by applying the LBRG transformation to the model (1). The horizontal surface at positive $\mathcal{J}_2$ separates the F phase at positive $\mathcal{J}_1$ from the AF phase. At lower values of $\mathcal{J}_2$ the F and the AF phases are separated by the P phase.

F phase at positive $\mathcal{J}_1$ as shown in figure 2. The model (1) exhibits the exact symmetry $\mathcal{J}_1 \to -\mathcal{J}_1$ [9]. This symmetry is not respected in figure 2. However, we observe that simple block transformations would completely miss the F–AF transition in the 2D version of the model (1) [25]. On the surface between the F and the AF phases we find the fixed point (D); it has one relevant eigenvalue given at $p = p_c^*$ by $\lambda = 2^{y_D}$ with $y_D = 2.724\,54$. We interpret the point (D) as a discontinuity fixed point related to the F–AF first-order transition, which should be characterized by the value $y_D = D = 3$ [26]. If we maximize the free energy with respect to the discontinuity fixed point, we get $y_D = 1.78$ at $p = 0.31$, which is the lowest value for which the discontinuity fixed point exists. The fact that this result is worse than the one obtained at $p = p_c^*$ can be explained by saying that the LBRG transformation does not give good results when not ferromagnetic ground states are involved.

Numerical simulations of [8, 9] show the existence of a line of tricritical points on the F–P transition surface close to the $\mathcal{J}_1 = 0$ plane; this line, at decreasing values of $\mathcal{J}_4$, ends in a Baxter point. Due to the limits of applicability of the LBRG transformation at small $\mathcal{J}_1$, we cannot give reliable predictions on the structure of the phase diagram in the region where the F–P and the AF–P surfaces meet. However, we have also studied the RG recursions on the line $\mathcal{L}$ separating the domains of attraction of the fixed points (C) and (D) on the surface $\mathcal{F}$. On the line $\mathcal{L}$, which is very close to the intersection of the AF–P with the $\mathcal{F}$ surface, we find a fixed point (L) with two relevant eigenvalues, which annihilates with the discontinuity fixed point for $p < 0.31$. The free energy of this fixed point is maximum at p very close to p_c^*, where the exponents of the two relevant eigenvalues are $y_1 = 1.593\,47$ and $y_2 = 0.095\,64$ [27]. The largest not relevant eigenvalue is $\lambda = 0.903\,95$. The fixed point (L) is also reported in table 1; it can be seen that it is very close to the fixed point (C).

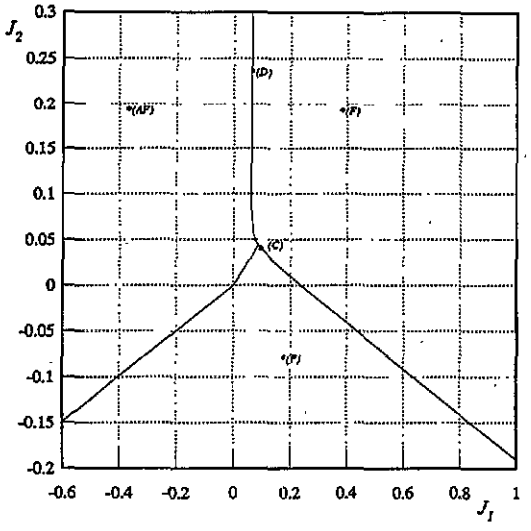

Figure 3. The phase diagram of the model (1) with $\mathcal{J}_2 = \mathcal{J}_4$. Fixed points of table 1 are also reported.

Table 2. *The critical values of β_S in the self-avoidness limit for different values of β_C. The* Monte Carlo results are taken from [8, 9].

β_C		0.04	0	−0.04	−0.1	−0.2
β_S	LBRG	0.446	0.472	0.504	0.560	0.674
	Monte Carlo	—	0.353[8]	0.360[9]	0.470[9]	0.570[9]

A realistic discussion of the phase diagram in the plane $\mathcal{J}_1 = 0$, where the F–P and the AF–P surfaces should meet, is given in [28].

In figure 3 the phase diagram is shown in the particular case $\mathcal{J}_4 = \mathcal{J}_2$, which means $\beta_C = 0$ in the surface representation. The paramagnetic phase, in accord with Monte Carlo results and differently from what comes out from mean-field approximation [9], extends at positive $\mathcal{J}_1$ towards zero temperature. This is related to the high degeneracy of the ground states in this region [9].

A different representation of the phase diagram can be given in terms of the surface parameters β_L, β_S and β_C (see equation (2)). In figure 4 the F–P–AF transitions are shown in the plane β_L, β_S for different values of the curvature β_C. The F phase, at large values of β_S, describes configurations with diluted small surfaces. By decreasing the value of β_S, area is favoured to increase and, at the percolation threshold, interfaces invade the system. However, it is still possible to distinguish between an *inside* volume wrapped up in interfaces and a different *outside* volume. By decreasing furtherly the value of β_S, if β_L is sufficiently large, at the Ising-like F–P transition, a *random isotropic* [29] phase is stable and the symmetry of the Hamiltonian between inside and outside is restored. The AF phase can be intended as a droplet crystal. The limit $\beta_L \to \infty$ describes a gas of self-avoiding surfaces and is particularly relevant for physics. In table 2 the critical values of β_S for self-avoiding surfaces are reported at different values of the curvature and compared with results from simulations.

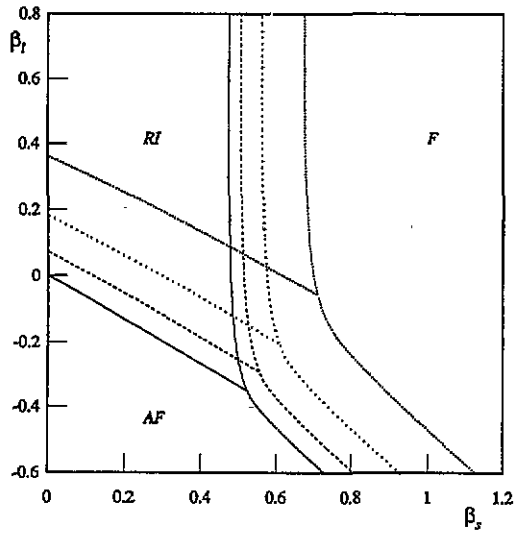

Figure 4. The phase diagram of the model (1) in terms of the surface parameters β_S and β_L. The different curves refer from the right to the left, respectively, to the values of $\beta_C = -0.2, -0.1, -0.04$ and 0. The symbols F, AF and RI denote, respectively, the ferromagnetic, the antiferromagnetic and the random isotropic or paramagnetic phase.

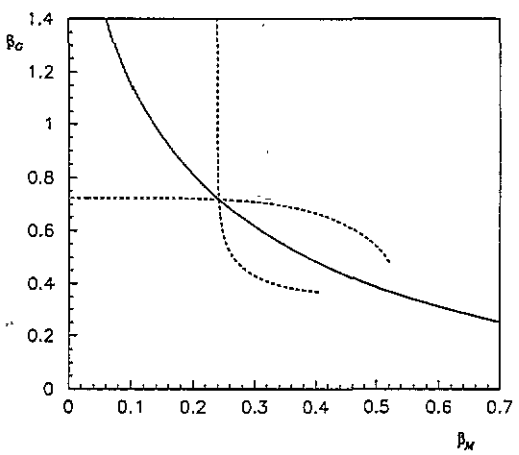

Figure 5. The phase diagram of the self-dual $Z(2)$ gauge model. The full curve is the self-dual line. The broken curves are critical lines found by applying the LBRG transformation to the model (5).

Open interfaces—model (3), (5)

The gauge model (3) at $\beta_M = 0$ is dual to the 3D Ising model [14]. At small β_M it can be expanded on the dual lattice as an Ising model with many interactions. At the second order of this expansion the gauge model is mapped onto the model (5). The LBRG transformation has been applied to study the F–P transition in the model (5). Then the results have been reported by the formulae (6) and (7) in the plane $\beta_M\beta_G$, as shown in figure 5. At small β_M the critical line starts from the β_G axis at $\beta_G = -\frac{1}{2}\ln\tanh\beta^I_{crit}$, with $\beta^I_{crit} = 0.239\,26$.

The full curve in figure 5 is the self-dual line, which is the line mapped onto itself by transformations (4), with respect to which the phase diagram has to be symmetric. Then the critical line at small β_M is mapped by (4) in the region at large β_G. The two curves meet at the point $\beta_M = 0.241$ and $\beta_G \models 0.719$ on the self-dual line. In the phase diagram found by numerical simulations [16], the two curves starting at $\beta_M = 0$ and at $\beta_G = \infty$ become first-order at tricritical points before meeting on the self-dual line. There, at a triple point, another first-order line comes out towards greater values of β_M on the self-dual line. This first-order line ends with a critical point at finite and positive values of β_G and β_M. As discussed in [17], an interesting aspect of the expansion (5) is that the four-spin interaction terms are expected to give tricritical points. However, a mean-field approximation of the model (5) [17] gives tricritical points quite far beyond the triple point. Also our calculations suggest that the transition lines are continuous on the parts drawn in figure 5, which correspond to the critical F–P transition in the Ising representation. Therefore, the relevance of the four-spin interaction in (5) is probably not sufficient to explain alone the existence of the tricritical points found in simulations. These results will be commented on further in the next section.

4. Discussions and conclusions

We have applied the LBRG transformation to study the phase diagram of Ising models describing closed and open interfaces. Interacting closed interfaces can be naturally expressed as an Ising model, while open surfaces, originally written as a gauge model with statistical variables on the bonds, can be mapped on Ising models only in extreme regions of the phase diagram. At large β_G, the gauge model describes the interesting physical situation of *almost*-closed surfaces with few defects.

First consider the model (1) of closed interfaces. Results concerning the transition on the nearest-neighbour axis are in good agreement with previous known results. Also the value of the Ising exponent $\nu = 0.6289$ is in excellent agreement with other numerical work. We expect that the critical surface has been found with a good approximation in the region close to the nearest-neighbour axis. Results regarding the interesting case of self-avoiding surfaces have been reported in table 2.

Problems arise when the LBRG transformation is applied to study regions of the phase diagram where ordered not ferromagnetic configurations are relevant. In particular, the LBRG transformation does not take into account the $\mathcal{J}_1 \to -\mathcal{J}_1$ symmetry of the model (1) which should give at low temperatures a first-order F–AF transition at $\mathcal{J}_1 = 0$. We find this first-order transition, but not at $\mathcal{J}_1 = 0$ (see figures 2 and 3). Moreover, our results cannot reliably describe the region close to the line where the F–P and the AF–P surfaces meet, which should be on the plane $\mathcal{J}_1 = 0$. However, for completeness, we have also given results concerning this region.

The model (1) has been largely studied in $D = 2$ [30], where RG transformations taking correctly into account the ground-state structure have been considered giving the expected topology of the phase diagram [28, 31]. We have tried to generalize the LBRG transformation in order to take into account the existence of antiferromagnetic ground states. Then we have considered a weight function $\mathcal{P}(\sigma', \sigma)$ distinguishing between spins of different sublattices. For each cell marked by a cross in figure 1 the spin σ' is coupled only to the four spins of one original sublattice (see equation (9) and figure 1), in such a way that two nearest neighbouring spins σ' are coupled to the spins σ of different sublattices. Then all the interaction is *moved* into the dark grey cells of figure 1 and a RG transformation analogous to (10) can be written in such a way to get a homogeneous Hamiltonian with

the same expression for any elementary cell. By this procedure we have obtained phase diagrams which exhibit the symmetry $\mathcal{J}_1 \to -\mathcal{J}_1$, but with a rather poor precision for the critical temperature on the nearest-neigbour axis and for the exponent ν. Moreover the tricritical points found numerically [9] close to the plane $\mathcal{J}_1 = 0$ are not obtained by this transformation. Therefore a complete RG study of the phase diagram of the model (1) in $D = 3$ is still an open question.

In figure 5 we have presented the phase diagram of the self-dual $Z(2)$ gauge model found by applying the LBRG transformation to the model (5). Our estimation of the critical lines is reliable especially in the region of validity of the expansion (5), that is at small β_M and, by duality, at large β_G, close to the points where the model can be written as an Ising model with only nearest-neighbour interaction. Numerical simulations [16] predict that these lines become first-order before meeting on the self-dual line. By our methods, we cannot predict such a behaviour. Indeed, our results suggest that the transition line remain continuous for a long part beyond the self-dual line. Therefore, even if tricritical points could arise in model (5), that expansion is probably not useful to discuss the phase diagram of the model (3) close to the self-dual line, for which other methods are needed. In conclusions, provided all the discussed limitations, we can say that the application of the LBRG transformation to spin models describing lattice interfaces gives, in a relatively simple way, phase diagrams in many parameter spaces which are quite accurate especially in the region close to the nearest-neighbour axis.

Acknowledgments

One of the authors (GG) thanks Professor Attilio Stella for a useful discussion about the subject of this work. We also thank Mr Alexis Pompili for having drawn figure 1.

References

[1] For a review on random surfaces models see, for example,
Nelson D R, Piran T and Weinberg S (eds) 1989 *Statistical Mechanics of Membranes and Surfaces* (Singapore: World Scientific)

[2] For a recent review see
Gommper G and Schick M 1994 Self-assembling amphiphilic systems *Phase Transitions and Critical Phenomena* ed C Domb and J L Lebowitz (New York: Academic)

[3] deGennes P G and Taupin C 1982 *J. Phys. Chem.* **86** 2294

[4] See, for example, Langevin D, Meunier J and Cazabat A 1985 *La Recherche* **16** 720

[5] See, for example, Porte G 1992 *J. Phys.: Cond. Matt.* 4 8649

[6] Intersections are intended as dual bonds where two pieces of surfaces touch each other. There are ambiguities in defining surfaces as boundaries between domains of opposite spins in Ising models (see, for example, Caselle M, Gliozzi F and Vinti S 1993 *Preprint* DFTT 12/93 and 1994 *Nucl. Phys.* B *Proc. Suppl.* 34 726). For example, imagine a local surface configuration of four plaquettes with a common bond. Excluded the possibility of self-intersections, you can cut and interpret this configuration in two different ways. It can be deduced [9] that, if $\mathcal{L}(\mathcal{C})$ is the total length of intersections in a configuration $\mathcal{C}$, there are $2^{\mathcal{L}(\mathcal{C})}$ possible interpretation of that configuration. However, these ambiguities will not be relevant for the following discussion (see [10]).

[7] Sterling T and Greensite J 1983 *Phys. Lett.* **121B** 345

[8] Karowski M 1986 *J. Phys. A: Math. Gen.* **19** 3375

[9] Cappi A, Colangelo P, Gonnella G and Maritan A 1992 *Nucl. Phys.* B **370** 659

[10] The ambiguities mentioned in [6] are practically overcome by saying that there is an energy cost β_L for each elementary intersection whatever is the surface interpretation of the intersection.

[11] Canham P B 1970 *J. Theor. Biol.* **26** 61
Helfrich W 1973 *Z. Naturf.* **28c** 693
See also Leibler S in [1]

[12] Colangelo P, Gonnella G and Maritan A 1993 *Phys. Rev.* E **47** 411
[13] Huse D A and Leibler S 1991 *Phys. Rev. Lett.* **66** 437
[14] Wegner F 1971 *J. Math. Phys.* **12** 2259
[15] Fradkin E and Shenker S H 1979 *Phys. Rev.* D **19** 3682
[16] Jongeward G A, Stack J D and Jayaprakash C 1980 *Phys. Rev.* D **21** 3360
[17] Gonnella G and van Leeuwen J M J *Phys. Rev.* E (to be published)
[18] A review of results concerning $Z(2)$ gauge models is given in
Drouffe J M and Zuber J B 1983 *Phys. Rep.* **102** 1
[19] Kadanoff L P 1975 *Phys. Rev. Lett.* **34** 1005
Kadanoff L P, Houghton A and Yalabik M C 1976 *J. Stat. Phys.* **14** 171; **15** 263
[20] For a review of results obtained by applying variational RG transformations, see
Burkhardt T W 1982 *Real Space Renormalization* ed T W Burkhardt and J M J van Leeuwen (Berlin: Springer)
[21] Burkhardt T W 1976 *Phys. Rev.* B **13** 3187
[22] For example, if $\mathcal{J}_1$ denotes the original nearest neighbour coupling, then $\mathcal{K}_1 = \mathcal{J}_1/4$, since each bond belongs to four different cells of the 3D lattice.
[23] Kadanoff L P 1976 *Ann. Phys., NY* **100** 359
[24] See, for example, Ferrenberg A M and Landau D P 1991 *Phys. Rev.* B **44** 5081 and references therein
[25] Nauenberg M and Neinhuis B 1974 *Phys. Rev. Lett.* **33** 944
[26] Nauenberg M and Neinhuis B 1975 *Phys. Rev. Lett.* **35** 477
[27] The expected values for the relevant exponents of a 3D tricritical fixed point are $y_1 = 2$, $y_2 = 1$, see
Wegner F J and Riedel E K 1973 *Phys. Rev.* B **7** 248
[28] van Leeuwen J M J 1975 *Phys. Rev. Lett.* **34** 1056
[29] Huse D A and Leibler S 1988 *J. Physique* **49** 605
[30] See, for example, Baxter R J 1989 *Exactly solved models in Statistical Mechanics* (New York: Academic)
[31] Nienhuis B, Sudbø A A S and Hauge E H 1978 *Physica* **92A** 222